ELSEVIER

Catalysis Today 51 (1999) 581–594

CATALYSIS TODAY

Electrochemical promotion of heterogeneous catalysis

Constantinos G. Vayenas*, Symeon Bebelis

Department of Chemical Engineering, University of Patras, GR-26500, Patras, Greece

Abstract

The catalytic activity and selectivity of metals interfaced with solid electrolytes can be altered dramatically and reversibly via potential application. The increase in catalytic rate can be several orders of magnitude higher than that anticipated from Faraday's Law. This new phenomenon of electrochemical promotion is of considerable theoretical and potentially practical importance in heterogeneous catalysis. In this paper the main phenomenological features of electrochemical promotion (or NEMCA effect) are surveyed and the origin of the effect is discussed in view of recent surface spectroscopic and quantum mechanical studies. © 1999 Elsevier Science B.V. All rights reserved.

Keywords: Electrochemical promotion; Heterogeneous catalysis; Solid electrolytes; NEMCA

1. Introduction

During the last three decades solid electrolyte fuel cells, operating on H_2 or CH_4 fuel, have been investigated extensively in order to assess their technical and economic viability for energy-efficient power generation [1,2]. The main commercial use of solid electrolyte cells is currently in sensor technology [3]. Wagner [4] was the first to propose the use of solid electrolyte cells in heterogeneous catalysis in order to measure the thermodynamic activity of oxygen in oxidation catalysts. This idea was pursued experimentally to study the mechanism of several catalytic systems [5]. It soon became apparent that solid electrolyte cells can also be used in an active mode to electrolyze molecules such as H_2O [6] and NO [7]. Another potential application of solid electrolyte cells is electrochemical cogeneration, i.e., the simultaneous production of electrical power and useful chemicals in fuel cell electrochemical reactors [8,9]. Such solid electrolyte fuel cells with modified anodes can be used, e.g., for the electrochemical oxidation of NH_3 to NO [8], H_2S to SO_2 [9], methanol to formaldehyde [10], or methane to ethylene [11] with simultaneous production (cogeneration) of chemicals and electricity.

In the course of chemical cogeneration studies a new and rather unexpected phenomenon was discovered, now known in the literature as non-Faradaic electrochemical modification of catalytic activity (NEMCA effect) or electrochemical promotion [12,13]. The NEMCA effect quickly attracted attention [14] and its importance in electrochemistry, catalysis and surface science has been stressed by Bockris [15], Haber [16] and Pritchard [14], respectively.

In brief, it was found that the catalytic activity and selectivity of metal films deposited on solid electrolytes (e.g. yttria-stabilized-zirconia (YSZ), an O^{2-}

*Corresponding author. Fax: +30-61-997269; e-mail: cat@zeus.chemeng.upatras.gr

PII: S0920-5861(99)00042-5

conductor, β''-Al_2O_3, a Na^+ conductor or $CaZr_{0.9}In_{0.1}O_{3-\alpha}$, a H^+ conductor) can be altered dramatically and reversibly by applying an electrical current or potential between the metal catalyst film and a second film (counter electrode) also deposited on the solid electrolyte.

The gaseous reactants (e.g. C_2H_4 plus O_2) are cofed over the working electrode of a solid electrolyte cell:

Gaseous reactants (e.g. $C_2H_4 + O_2$)	Catalyst working electrode (e.g. Pt, Rh, Ag, IrO_2)	Solid electrolyte (e.g. $ZrO_2-Y_2O_3$)	Counter electrode (e.g. Au)	Auxiliary gas (e.g. O_2)

The working electrode serves both as an electrode and as the catalyst for the catalytic (no net charge transfer) reaction, e.g.:

$$C_2H_4 + 3O_2 \rightarrow 2CO_2 + 2H_2O$$

The auxiliary gas can be ambient air when using the 'fuel cell' type design (Fig. 1, top) or the reactive gas mixture itself, in the so called 'single pellet' design [17].

The induced reversible change in catalytic rate (expressed in mol/s) was found to be up to 100 times larger than the catalytic rate before current application, i.e., there is up to a 10 000% rate increase. Furthermore, this rate increase is typically 10–10^5 times larger than the rate, I/nF, of supply of ions (e.g. O^{2-}, Na^+, H^+) to the catalyst surface (where I is the applied current, n the ion charge and F is Faraday's constant). This implies that each ion supplied to the catalyst can cause up to 10^5 adsorbed reactants to react and produce up to 10^5 product molecules: electricity acts as a powerful promoter rather than only an electrochemical driver of catalytic activity. Importantly, significant and reversible alterations in product selectivity were also observed for several reactions and it soon became apparent that the NEMCA effect is not limited to any particular metal catalyst, solid electrolyte or catalytic reaction. By 1992 when the NEMCA literature was first reviewed [17] more than 20 catalytic reactions exhibiting the novel effect had been studied.

Today this number has exceeded 50 [18] and the effect has been demonstrated for several catalysts (Pt, Pd, Rh, Ag, Ni, Au, IrO_2, RuO_2) deposited on O^{2-}, F^-, Na^+ and H^+ conducting solid electrolytes. Recent demonstration of NEMCA using mixed ionic–electronic conductors (e.g. TiO_2) [19], Nafion [20] or aqueous alkaline solutions [21] is also noteworthy. In addition to the group which first reported on this effect [12,13,17,18], several other research groups at Novosibirsk [22], Yale [23], Cambridge [24], Tufts [25] and EPFL [26] have made important contributions in this area.

In this paper the main phenomenological features of electrochemical promotion are surveyed and the origin of the effect is discussed in the light of kinetic, electrokinetic, surface spectroscopic and quantum mechanical investigations.

2. Experimental

The basic experimental setup for kinetic–electrokinetic studies is shown schematically in Fig. 1(a). The electronically conductive working catalyst electrode, usually in the form of a porous film 3–20 μm in thickness with a roughness factor 3–500 [17,18,27] is deposited on the surface of a ceramic solid electrolyte (e.g. Y_2O_3-stabilized-ZrO_2 (YSZ), an O^{2-} conductor, Na-β''-Al_2O_3, a Na^+ conductor, $CaZr_{0.9}In_{0.1}O_{3-\alpha}$, a H^+ conductor [28], or TiO_2, a mixed electronic–ionic conductor [19]). Catalyst, counter and reference electrode preparation and characterization details have been presented in detail elsewhere [17,18] together with the gas analysis system for on-line monitoring the rates of catalytic reactions via gas chromatography, mass spectrometry and infrared spectroscopy.

The superficial surface area of the metal working electrode–catalyst is typically 1–2 cm^2 while the true surface areas are typically between 50 and 2000 cm^2, as measured via reactive titration of oxygen with CO or C_2H_4 or via reactive titration of CO with O_2 [17,18]. The catalyst–electrode is exposed to the reactive gas mixture (e.g. C_2H_4+O_2) in a continuous flow gradientless reactor (CSTR). The counter and reference electrodes are usually exposed to air when using the ''fuel

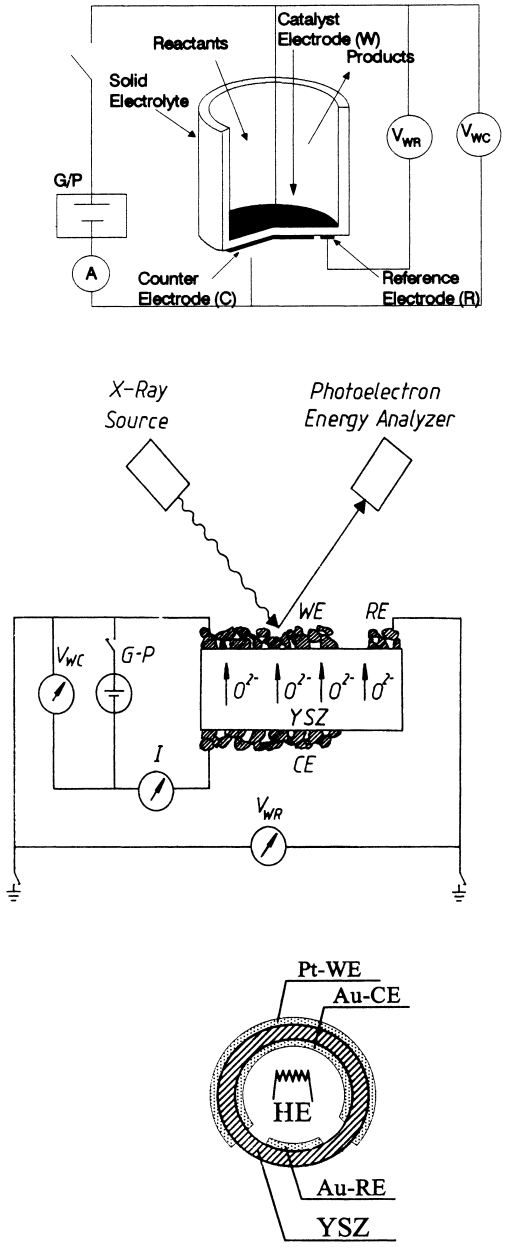

Fig. 1. Schematic of the experimental setup for electrochemical promotion studies using the fuel-cell type design (a) and for using X-ray photoelectron spectroscopy (XPS) (b) and temperature-programmed desorption (TPD) (c) to investigate the catalyst–electrode surface; G–P: galvanostat–potentiostat; WE: working electrode, RE: reference electrode, CE: counter electrode; HE: heating element (adapted from [18,43,34]).

cell'' type design and to the reactive gas mixture itself when using the ''single-pellet'' type design. In the latter case the counter and reference electrodes must be catalytically inert (e.g. Au) while the reference electrode is only a monitoring (pseudoreference) electrode [30].

A galvanostat or potentiostat is used to apply constant currents between the catalyst and counter elec-

trode or constant potentials, V_{WR}, between the catalyst-working electrode (W) and the reference (R) electrode. In this way ions (O^{2-} in the case of YSZ, Na^+ in the case of β''-Al_2O_3, H^+ in the case of $CaZr_{0.9}In_{0.1}O_{3-\alpha}$) are supplied from (or to) the solid electrolyte to (or from) the catalyst–electrode surface. The current, I, is defined positive when anions are supplied to or cations removed from the catalyst surface. As shown under Section 3 there is concrete evidence obtained from several techniques, including work function measurements, cyclic voltammetry, temperature-programmed desorption (TPD), X-ray photoelectron-spectroscopy (XPS) and scanning tunneling microscopy (STM) that these ions (accompanied by their compensating (screening) charge in the metal thus forming surface dipoles) migrate (backspillover in the catalytic terminology) onto the gas-exposed, i.e. catalytically active, catalyst–electrode surface. Consequently the electrolyte acts as an electrically activated catalyst support and establishes an ''effective electrochemical double layer'' on the gas-exposed, i.e. catalytically active, electrode surface.

The experimental setups and procedures for using XPS [31–33], TPD [34] and cyclic voltammetry [35] under ultra-high-vacuum (UHV) conditions and work function measurements [13,36], cyclic voltammetry [34,35] and STM [37] under atmospheric pressure conditions to investigate the origin of electrochemical promotion, as shown schematically in Fig. 1 have been described in detail in the corresponding recent publications [13,31–37].

3. Results and discussion

3.1. Catalytic rate modification

A typical transient NEMCA experiment, carried out in the setup depicted in Fig. 1(a), is shown in Fig. 2. The solid electrolyte is YSZ. The catalytic reaction is the complete oxidation of C_2H_4 on Pt [38]. The Pt catalyst film has a gas exposed surface area corresponding to $N=4.2\times10^{-9}$ mol Pt and is exposed to $P_{O_2}=4.6$ kPa, $P_{C_2H_4}=0.36$ kPa, $T=370^\circ$C in the gradientless continuous flow CSTR reactor of Fig. 1(a). Initially ($t<0$) the electrical circuit is open ($I=0$) and the open-circuit catalytic rate, r_o, is 1.5×10^{-8} mol O/s. The corresponding turnover frequency (TOF), i.e., oxygen atoms reacting with C_2H_4 per surface Pt site per second is 3.57 s^{-1}.

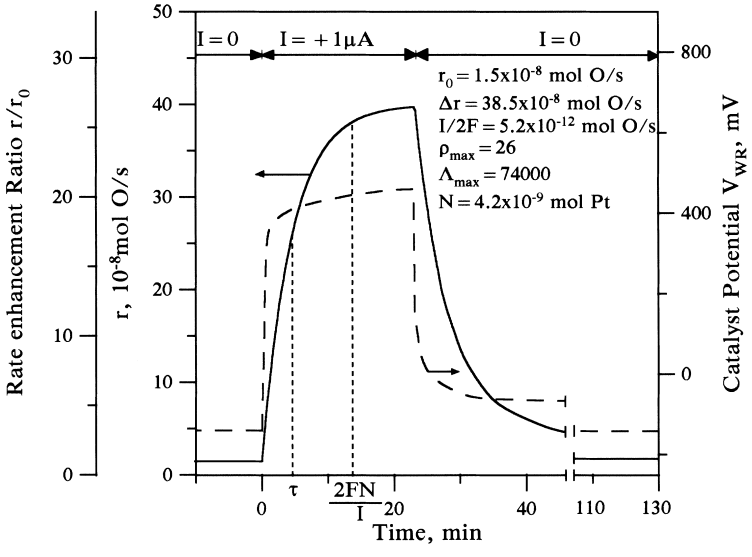

Fig. 2. Electrochemical promotion: catalytic rate and catalyst potential response to step changes in applied current during C_2H_4 oxidation on Pt [38]. $T=370^\circ$C, $P_{O_2}=4.6$ kPa, $P_{C_2H_4}=0.36$ kPa. The experimental (τ) and computed ($2FN/I$) rate relaxation time constants are shown on the figure. The steady-state rate increase Δr is 74 000 times higher than the steady-state rate of supply of O^{2-} to the catalyst-electrode ($\Lambda=74\,000$); (adapted from [38]).

Then at $t=0$ a galvanostat is used to apply a constant current between the catalyst and the counter electrode. In this way oxygen ions, O^{2-}, are supplied to the catalyst–gas–solid electrolyte three-phase boundaries (TPB) at a rate $I/2F=5.2\times10^{-12}$ mol O/s. The catalytic rate starts increasing (Fig. 2) and within 25 min gradually reaches a value $r=4.0\times10^{-7}$ mol O/s which is 26 times larger than r_o. The new TOF is 95.2 s^{-1}. The increase in catalytic rate $\Delta r=r-r_o=3.85\times10^{-7}$ mol O/s is 74 000 times larger than $I/2F$, which is the maximum rate increase anticipated from Faraday's Law. Thus each O^{2-} ion supplied to the Pt catalyst causes at steady-state 74 000 oxygen atoms chemisorbed on the Pt surface to react with C_2H_4 and form CO_2 and H_2O. This is why this novel effect has been termed non-Faradaic electrochemical modification of catalytic activity (NEMCA effect).

The Faradaic efficiency, or enhancement factor, Λ, is defined [17,18] from the following equation:

$$\Lambda = \Delta r/(I/2F). \tag{1}$$

where r is expressed in mol O/s

For the experiment of Fig. 2 the maximum Λ value is 74 000. A reaction exhibits NEMCA when $|\Lambda|>1$. Depending on the observed sign of Λ, catalytic reactions are termed electrophobic ($\Lambda>1$) or electrophilic ($\Lambda<-1$); Λ values ranging from 3×10^5 [17,18] and down to -5×10^4 [17,18] have been measured. More important, relatively safe predictions can be made about the order of magnitude of Λ as discussed below.

The rate enhancement ratio, ρ, is defined from the following equation:

$$\rho = r/r_o. \tag{2}$$

For the experiment of Fig. 2, the maximum ρ value is 26; ρ values up to 100 [39] or even higher [24] and down to 0 [40–42] have been obtained.

The NEMCA rate relaxation time constant, τ, is defined [17,18] as the time required for the catalytic rate increase to reach 63% of its final steady-state value in galvanostatic transient experiments, such as the one depicted in Fig. 2. As shown in this figure, τ is of the order of $2FN/I$ and this turns out to be a general observation in NEMCA studies utilizing YSZ:

$$\tau \approx 2FN/I. \tag{3}$$

The parameter $2FN/I$ denotes the time required to form a monolayer of O on a surface with N adsorption sites, when O is supplied as O^{2-} at a rate $I/2F$ as is the case here. This provided the first, kinetic, evidence that NEMCA is due to the electrochemically controlled migration (backspillover) of oxygen from the solid electrolyte onto the gas-exposed catalytically active catalyst surface. As shown below via XPS, TPD and cyclic voltammetry this electrochemically supplied oxygen forms a new strongly bound ionic adsorption state on the Pt surface and is far less reactive than normally chemisorbed oxygen formed via gas phase adsorption. It severely modifies (increases) the catalyst surface work function [13,36], forces normally chemisorbed oxygen into a weakly bonded adsorption state [34] and acts as a sacrificial promoter by reacting with C_2H_4 (or other reactive molecules) at a rate Λ times slower than the weakly bonded atomic oxygen [34,36].

This is already manifest in Fig. 2: at steady-state the rate, r_c, of consumption of the promoting O^{2-} species via reaction with C_2H_4, has to equal its rate of formation $I/2F$. Consequently, since $\Lambda=\Delta r/(I/2F)$ and $\Delta r\approx r$, it follows $\Lambda=r/r_c=\mathrm{TOF}/\mathrm{TOF}_c$ where TOF is the turnover frequency of the catalytic reaction in the NEMCA-promoted state and TOF_c is the turnover frequency of the reaction of the promoting oxygen species with ethylene. It thus follows for the experiment of Fig. 2 that $TOF_c=TOF/\Lambda=1.3\times10^{-3}$ s. This implies that the average lifetime of the promoting species on the catalyst surface is TOF_c^{-1} in excellent qualitative agreement with the catalytic rate relaxation time constant upon current interruption (Fig. 2.). This observation provides strong and conclusive support for the oxygen backspillover mechanism.

Similar observations can be made in Fig. 3 which presents a galvanostatic transient during ethylene oxidation on Rh/YSZ [29]. Here the rate increases reversibly by a factor of 88 with a Λ value of 770.

Fig. 4 shows the steady-state effect of applying a constant positive potential $V_{WR}(=+1V)$ on the rate of C_2H_4 oxidation on Pt/YSZ as a function of the $P_{O_2}/P_{C_2H_4}$ ratio. The NEMCA effect is much more pronounced under oxidizing gaseous compositions, where a sixtyfold enhancement in catalytic rate and turnover frequency is obtained. The stronger electrochemical enhancement under oxidizing conditions is a general observation in NEMCA studies of oxidation reactions [17,18] and is due to the fact that the promoting ionic oxygen species forms, upon O^{2-}

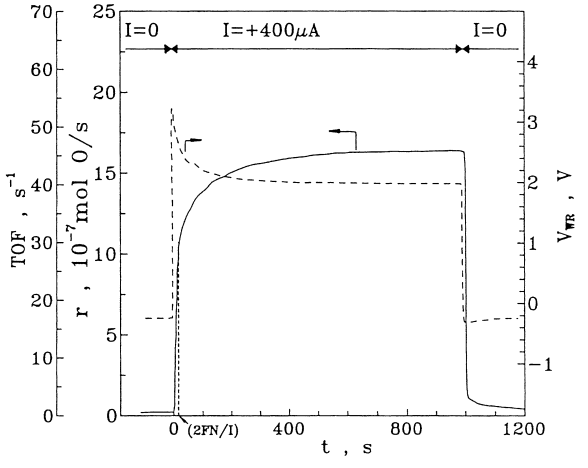

Fig. 3. NEMCA: rate and catalyst potential response to step changes in applied current during C_2H_4 oxidation on Rh. T=350°C, P_{O_2}=2.6 kPa, $P_{C_2H_4}$=5.9 kPa, $r_o=1.8\times10^{-8}$ mol O/s, $\Delta r=1.6\times10^{-6}$ mol O/s, $I/2F=2.1\times10^{-9}$ mol O/s, Λ=770, ρ=88 (reprinted with permission from [29]).

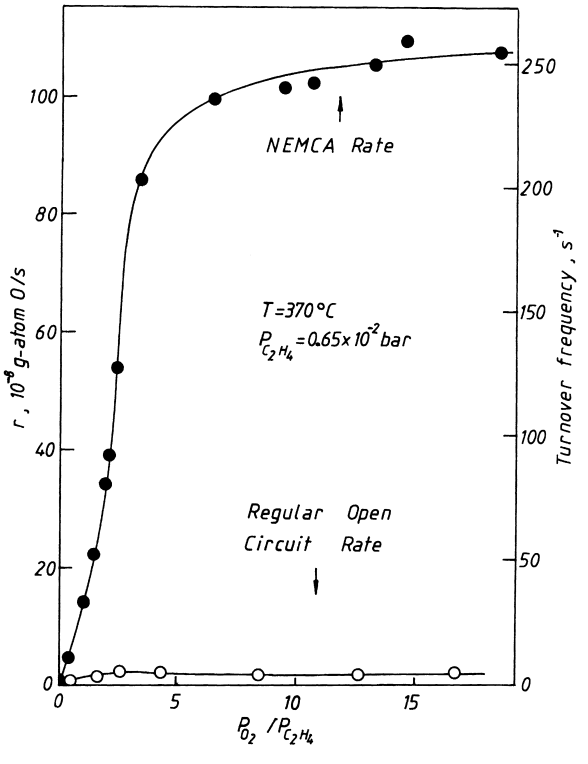

Fig. 4. Effect of gaseous composition on the open-circuit (unpromoted) catalytic rate of C_2H_4 oxidation on Pt/YSZ and on the electrochemically promoted catalytic rate when the Pt catalyst film is maintained at V_{WR}=1V (adapted from [38]).

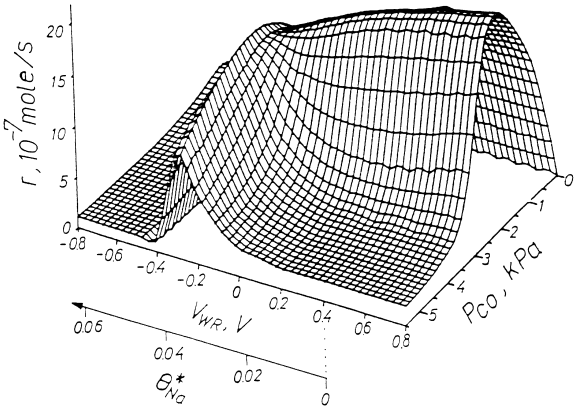

Fig. 5. Electrochemical promotion of Pt for CO oxidation using Na–β″-Al_2O_3: effect of P_{CO}, catalyst potential and corresponding linearized sodium coverage on the rate of CO oxidation at T=350°C and P_{O_2}=6 kPa (reprinted with permission from [44]).

supply, only after the coverage of normally adsorbed oxygen is near completion [34,43].

Fig. 5 provides an example of using Na- β″-Al_2O_3, a Na^+ conductor, as the solid electrolyte to induce NEMCA. The figure depicts the effect of catalyst potential V_{WR}, corresponding coulometrically measured [42,44] Na coverage θ_{Na}, and P_{CO} on the rate of CO oxidation on Pt/Na- β″-Al_2O_3 at 350°C [44]. When the Pt surface is Na-free, the rate goes through a sharp maximum with respect to P_{CO}, indicative of competitive adsorption of CO and O (Langmuir–Hinshelwood type kinetics). For high P_{CO} values the surface coverage of O is very low and thus the catalytic rate is also low. Increasing Na coverage (via negative current or potential application) under these conditions causes a sixfold enhancement in the rate of CO oxidation due to Na-assisted enhanced O chemisorption. The promotion index of Na, P_{Na}, defined from:

$$P_{Na} = (\Delta r/r_o)/\Delta\theta_{Na} \quad (4)$$

is up to 200 under these conditions. Higher Na coverages (Fig. 5) poison the rate due to the formation of surface Na–CO complexes [44].

3.2. Selectivity modification

Electrochemical promotion can be used to modify significantly the product distribution, i.e. the selectivity, of catalytic reactions. An example is shown in

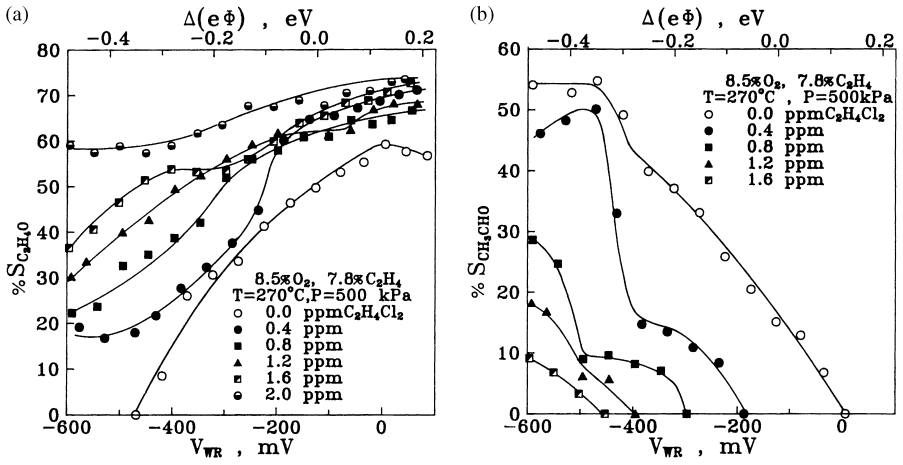

Fig. 6. Effect of catalyst potential and work function and of the gas-phase addition of various levels of 1,2-$C_2H_4Cl_2$ on the selectivity to ethylene oxide (a) and acetaldehyde (b) of ethylene oxidation on Ag supported on YSZ (reprinted with permission from [41]).

Fig. 6 which presents the effect of catalyst potential and corresponding work function change on the selectivity to ethylene oxide (Fig. 6(a)) and acetaldehyde (Fig. 6(b)) of ethylene oxidation on Ag/YSZ at various levels of gas phase chlorinated hydrocarbon moderators [41] (the third, undesirable, product is CO_2). As shown in the figure a 500 mV decrease in catalyst potential causes the Ag surface to change from selective (up to 70%) ethylene oxide production to selective (up to 55%) acetaldehyde production. The same study [41] has shown that the total rate of ethylene oxidation varies by a factor of 200 upon varying the catalyst potential.

Fig. 7 shows the effect of catalyst potential on the selectivity to ethylene oxide at various levels of gas phase chlorinated hydrocarbon moderator when β''-Al_2O_3 is used as the solid electrolyte [45]. In this case ethylene oxide selectivity up to 88% is obtained.

The dramatic effect of catalyst potential on product selectivity is shown in Fig. 8 for the environmentaly important reduction of NO by CO on Pt supported on β''-Al_2O_3 [46]. Lowering the catalyst potential to negative values, i.e. supplying sodium to the catalyst surface causes a pronounced increase in the rates of CO_2, N_2 and N_2O production and a threefold enhancement in the product selectivity to N_2. This is one of the rare cases where a single promoter enhances both the rate and the selectivity to the desired product. This pronounced increase in catalyst activity and selectivity is due to enhanced NO dissociation on the Pt surface [46]. Similar behavior has been observed in studies of NO reduction by H_2 [47], C_2H_4 [48] and C_3H_6 [33] on Pt and Pd [49] using either β''-Al_2O_3 or YSZ as the solid electrolyte, upon negative potential application.

3.3. *Exchange current density and the magnitude of the Faradaic efficiency*

Table 1 provides a list of the catalytic reactions studied so far from the view point of electrochemical

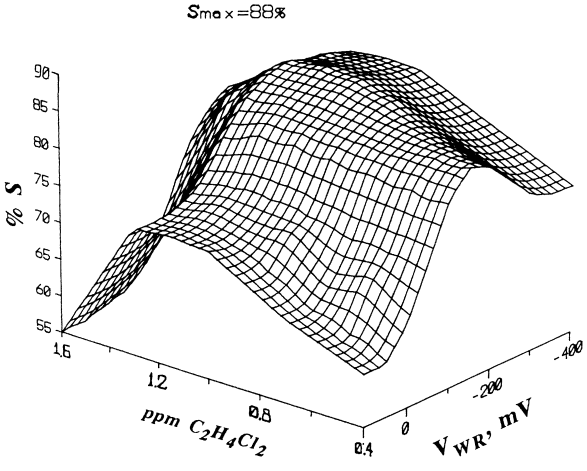

Fig. 7. Effect of catalyst potential and of gas-phase 1,2-$C_2H_4Cl_2$ partial pressure on the selectivity of ethylene epoxidation on Ag/β''-Al_2O_3. T=260°C; P=500 kPa, 4% O_2, 13%C_2H_4 (reprinted with permission from [45]).

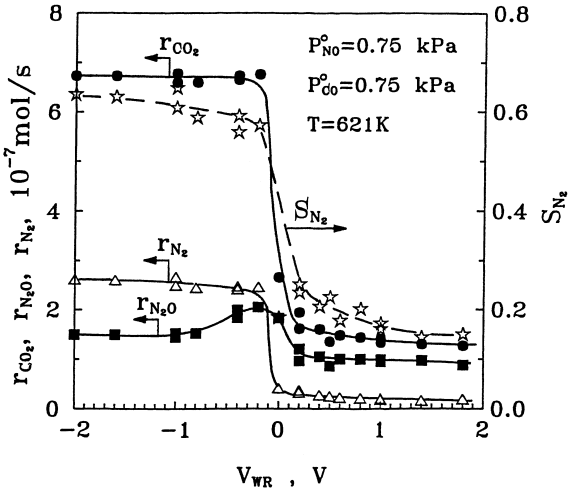

Fig. 8. Effect of catalyst potential (V_{WR}) on the CO_2, N_2, N_2O formation rates and the selectivity of NO reduction to nitrogen. Conditions: T=621 K, $P^o_{NO} = P^o_{CO} = 0.75$ kPa (reprinted with permission from [46]).

promotion and of the measured Λ, ρ and P_i values. As shown in this table the measured $|\Lambda|$ values range from 1×10^5 to 3×10^5. It has been shown both theoretically and experimentally [17,18] that the order of magnitude of the absolute value $|\Lambda|$ of the Faradaic efficiency Λ can be estimated for any reaction, catalyst and solid electrolyte from the approximate expression:

$$|\Lambda| = r_o/(I_0/2F), \tag{5}$$

where r_o is the open-circuit catalytic rate and I_0 is the exchange current of the catalyst–solid electrolyte interface. The latter can be obtained from standard current–overpotential (Tafel) plots [17,18]. Eq. (5) underlines that in order to obtain a non-Faradaic rate enhancement ($|\Lambda|>1$) it is necessary, and as far as we know sufficient, that the intrinsic catalytic rate, r_o, must be higher than the intrinsic electrocatalytic rate $I_0/2F$.

3.4. Work function measurements

A key step in the understanding of the origin of NEMCA was the realization that solid electrolyte cells with metal electrodes are both work function probes and work function controllers for the gas-exposed surfaces of their electrodes [13,36]. It was shown both theoretically [17,18] and experimentally via the Kelvin probe (vibrating capacitor) technique [13,36] and more recently via UPS [50] that:

$$eV^o_{WR} = e\Phi_W - e\Phi_R \tag{6}$$

and

$$e\Delta_{WR} = \Delta(e\Phi_W), \tag{7}$$

where $e\Phi_W$ is the catalyst surface work function and $e\Phi_R$ is the work function of the reference electrode surface.

Eq. (6) provides a new and important physical meaning to the EMF, V^o_{WR}, of solid electrolyte cells, in addition to its common Nernstian meaning [17,18]. Eq. (7) is equally important as it shows that the work function of the gas-exposed, i.e., catalytically active, surface of solid electrolyte cell electrodes can be varied at will by up to at least 1 eV [13,36,50] via current or potential application. Positive currents increase $e\Phi$ and negative currents decrease it. Physically this variation is brought about at the molecular level by the spillover of ions from or to the electrolyte to or from the catalyst surface [18].

3.5. XPS investigation

X-ray photoelectron spectroscopy (XPS) has provided concrete evidence that spillover/backspillover phenomena are real and that electrochemically controlled backspillover of oxide ions, $O^{\delta-}$, is the origin of electrochemical promotion. The first XPS investigation of Ag electrodes on YSZ under electrochemical O^{2-} pumping conditions was published in 1983 [31] and provided direct evidence for the creation of backspillover oxide ions on Ag (O1s at 529.2 eV) upon positive current application. These findings were confirmed by Göpel and coworkers [50] who used XPS, UPS and EELS to study Ag/YSZ catalyst surfaces under electrochemical bias.

A similar detailed XPS study of Pt films interfaced with YSZ [43] has shown conclusively that:

1. Backspillover oxide ions (O1s at 528.8 eV) are generated on the gas-exposed Pt electrode surface upon positive current application (peak δ in Fig. 9 top).
2. Normally chemisorbed atomic oxygen (O1s at 530.2 eV) also forms upon positive current appli-

Table 1
Catalytic reactions investigated in electrochemical promotion studies[a]

Reactants	Products	Catalyst	Electrolyte (promoting ion)	T (°C)	Λ	ρ	P_i
Electrophobic reactions $\partial r/\partial(e\Phi)>0$; $\partial r/\partial V_{WR}>0$; $\partial r/\partial I>0$; $\Lambda>0$							
C_2H_4, O_2	CO_2	Pt	YSZ (O^{2-})	260–450	3×10^5	55	55
C_2H_4, O_2	CO_2	Rh	YSZ (O^{2-})	250–400	5×10^4	90	90
C_2H_4, O_2	CO_2	IrO_2	YSZ (O^{2-})	350–400	200	6	5
C_2H_4, O_2	C_2H_4O, CO_2	Ag	YSZ (O^{2-})	320–470	300	30[b]	30
C_2H_6, O_2	CO_2	Pt	YSZ (O^{2-})	270–500	300	20	20
C_3H_6, O_2	C_3H_6O, CO_2 CO_2	Ag	YSZ (O^{2-})	320–420	300	2[b]	1
CH_4, O_2	CO_2	Pt	YSZ (O^{2-})	600–750	5	70	70
CH_4, O_2	CO_2	Pt	YSZ (O^{2-})	590	50	3	3
CH_4, O_2	CO_2,C_2H_4,C_2H_6	Ag	YSZ (O^{2-})	650–850	5	30[b]	30
CO, O_2	CO_2	Pt	YSZ (O^{2-})	300–550	2×10^3	3	2
CO, O_2	CO_2	Pd	YSZ (O^{2-})	400–550	10^3	2	1
CO, O_2	CO_2	Ag	YSZ (O^{2-})	350–450	20	5	4
CH_3OH, O_2	H_2CO,CO_2	Pt	YSZ (O^{2-})	300–500	10^4	4[b]	3
CO_2, H_2	CH_4, CO	Rh	YSZ (O^{2-})	300–450	200	3[b]	2
CO, H_2	$C_xH_yC_xH_yO_z$	Pd	YSZ (O^{2-})	300–370	10	3[b]	2
CH_4, H_2O	CO, CO_2	Ni	YSZ (O^{2-})	600–900	12	2[b]	1
H_2S	S_x, H_2	Pd	YSZ (O^{2-})	600–750	–	11	10
C_2H_4, O_2	CO_2	Pt	β''-Al_2O_3(Na^+)	180–300	5×10^4	0.25	−30
CO, O_2	CO_2	Pt	β''-Al_2O_3(Na^+)	300–450	10^5	0.3	−30
C_6H_6, H_2	C_6H_{12}	Pt	β''-Al_2O_3(Na^+)	100–150	–	∼0	−10
CH_4	C_2H_6, C_2H_4	Ag	$SrCe_{0.95}Yb_{0.05}O_3$(H^+)	750	–	11[b]	10
C_2H_4, H_2	C_2H_6	Ni	$CsHSO_4$(H^+)	150–170	6–300	0.16–2	12
H_2, O_2	H_2O	Pt	Nafion (H^+)	25	20	6	5
H_2, O_2	H_2O	Pt	KOH-H_2O (OH^-)	25–50	20	6	5
CO, O_2	CO_2	Pt	CaF_2(F^-)	500–700	200	2.5	1.5
C_2H_4, O_2	CO_2	Pt	TiO_2(TiO_x^+, O^{2-})	450–600	5×10^3	20	20
Electrophilic reactions $\partial r/\partial(e\Phi)<0$; $\partial r/\partial V_{WR}<0$; $\partial r/\partial I<0$; $\Lambda<0$							
C_2H_6, O_2	CO_2	Pt	YSZ (O^{2-})	270–500	−100	7	–
C_3H_6, O_2	CO_2	Pt	YSZ (O^{2-})	350–480	-3×10^3	6	–
CO, O_2	CO_2	Pt	YSZ (O^{2-})	300–550	−500	6	–
CO, O_2	CO_2	Au	YSZ (O^{2-})	450–600	−60	3	–
CO_2, H_2	CO	Pd	YSZ (O^{2-})	500–590	−50	10	–
CH_3OH, O_2	H_2CO, CO_2	Pt	YSZ (O^{2-})	300–550	-10^4	15[b]	–
CH_3OH	H_2CO, CO, CH_4	Ag	YSZ (O^{2-})	550–750	−25	6[b]	–
CH_3OH	H_2CO, CO, CH_4	Pt	YSZ (O^{2-})	400–500	−10	3[b]	–
CH_4, O_2	CO_2	Au	YSZ (O^{2-})	700–750	−3	3[b]	–
CH_4, O_2	C_2H_4, C_2H_6, CO_2	Ag	YSZ (O^{2-})	700–750	−1.2	8[b]	–
CO, O_2	CO_2	Pt	β''-Al_2O_3(Na^+)	300–450	-10^5	8	250
C_2H_4, NO	CO_2, N_2, N_2O	Pt	β''-Al_2O_3(Na^+)	400	–	∞	500
CO, NO	CO_2, N_2, N_2O	Pt	β''-Al_2O_3(Na^+)	320–400	–	13[b]	200

[a] Adapted from Table 3 in ref. [18] which provides specific references to each reaction.
[b] Promotion-induced change in product selectivity.

cation (peak γ in Fig. 9 top). The maximum coverages of the γ and δ states are comparable and of the order of 0.5 each.

3. Oxidic backspillover oxygen (δ-state) is significantly less reactive with the reducing (H_2 and CO) ultra high vacuum background than normally

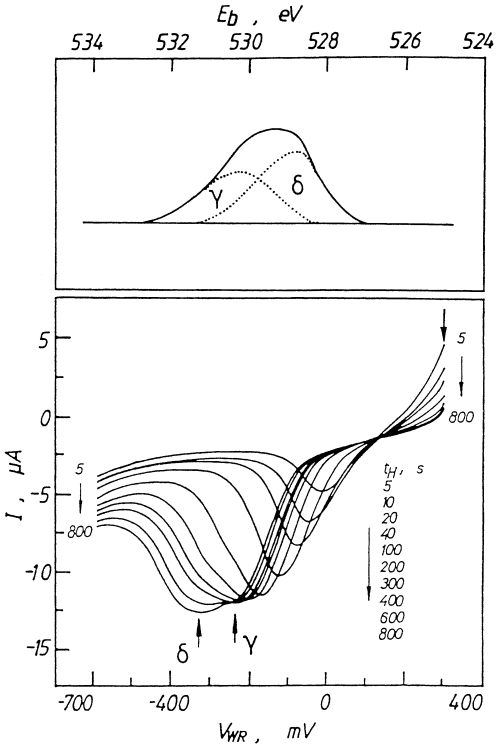

Fig. 9. XPS (top) and linear potential sweep voltammographic (bottom) investigation of oxygen adsorbed on Pt films deposited on YSZ following positive overpotential application. Top: O1s photoelectron spectrum of oxygen adsorbed on a Pt electrode supported on YSZ under UHV conditions after applying a constant overpotential ΔV_{WR}=1.2 V, corresponding to a steady-state current I=40 μA for 15 min at 673 K [43]. The same O1s spectrum is maintained after turning off the potentiostat and rapidly cooling to 400 K [43]. The γ-state is normally chemisorbed atomic oxygen (E_b=530.2 eV) and the δ-state is backspillover oxidic oxygen (E_b=528.8 eV). Bottom: linear potential sweep voltammogram obtained at T=653 K and P_{O_2}=0.1 kPa on a Pt electrode supported on YSZ showing the effect of holding time t_H at V_{WR}=300 mV on the reduction of the γ- and δ- states of adsorbed oxygen; sweep rate: 30 mV/s [52].

chemisorbed atomic oxygen. These observations provide a direct explanation of electrochemical promotion when using O^{2-}-conducting solid electrolytes [43].

The use of XPS has also recently confirmed that electrochemically controlled Na backspillover is the origin of electrochemical promotion when using Na^+-conducting solid electrolytes such as β″-Al_2O_3 [24,33,51].

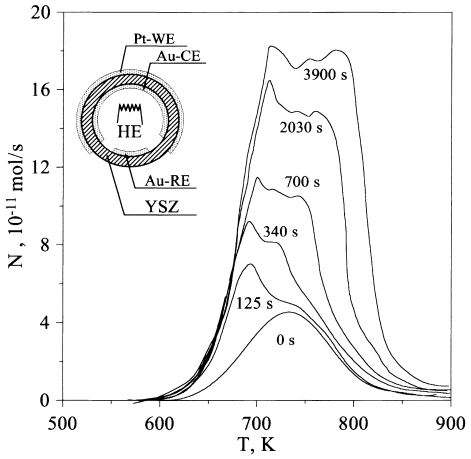

Fig. 10. Oxygen TPD spectra after gaseous oxygen adsorption at 673 K and $P_{O_2}=4\times10^{-6}$ Torr for 1800 s (7.2 kL) followed by electrochemical O^{2-} supply (I=15 μA) for various time periods t/s comparable to 2FN/I (2570 s). Gaseous oxygen supply creates a single adsorption state (T_p=740 K), but additional electrochemical oxygen supply creates two adsorption states. The weakly bonded state is highly reactive [34], while the strongly bonded (backspillover) state (T_p=750–780 K) acts as a sacrificial promoter for catalytic oxidations [34]. (Adapted from [34]).

3.6. Cyclic voltammetry

The dual nature of electrochemically generated chemisorbed oxygen on Pt films interfaced with YSZ is also clearly manifest via linear potential sweep voltammetry (Fig. 9 bottom, [52]): the first oxygen reduction peak corresponds to normally chemisorbed oxygen (γ-state) and the second reduction peak which appears only after prolonged positive current application [52] corresponds to the δ-state of oxygen, i.e. backspillover oxidic oxygen.

3.7. Temperature-programmed desorption

The creation of two types of chemisorbed oxygen on Pt surfaces interfaced with YSZ and subject to electrochemical promotion conditions is also manifest clearly by temperature-programmed desorption (TPD) [34] as shown in Fig. 10. The strongly bonded backspillover oxygen species (peak desorption temperature T_p=750–780 K) displaces the normal chemisorption state of atomic oxygen obtained via gas phase adsorption (T_p=740 K) to a significantly more weakly bonded state (T_p=680 K). The pronounced rate

enhancement in NEMCA studies of catalytic oxidations with positive potentials (electrophobic behavior) is due to the very fast oxidative action of this weakly bonded oxygen. The strongly bonded backspillover anionic oxygen is significantly (Λ times) less reactive and acts as a sacrificial promoter during catalytic oxidations.

3.8. Scanning tunneling microscopy (STM)

The most lucid demonstration of ion backspillover as the cause of NEMCA when using Na- β''-Al_2O_3 as the solid electrolyte was recently obtained with atmospheric pressure scanning tunneling microscopy (STM) (Fig. 11). A Pt monocrystal with an exposed Pt(1 1 1) surface was interfaced with a Na- β''-Al_2O_3 component using a Pt paste electrode along the perimeter [37]. Negative current application causes Na backspillover on the Pt(1 1 1) surface (Fig. 11, bottom) which actually at low surface coverage (<0.01) forms a Pt(1 1 1)–(12×12)–Na adlattice on the previously existing Pt(1 1 1)–(2×2)–O adlattice. Positive current application totally removes the Na adlattice leaving the Pt(1 1 1)–(2×2)–O adlattice intact (Fig. 11, top).

In addition to explaining NEMCA with Na^+-conducting solid electrolytes, this is the first STM confirmation of spillover/backspillover phenomena.

3.9. Ab initio quantum-mechanical calculations

An important feature of electrochemical promotion is the observed linear variation of catalytic activation energies with varying catalyst work function [17,18,27,38]. It had been proposed that this is due to a linear variation in chemisorptive bond strengths with catalyst work function [17,18], a proposition recently confirmed by TPD studies for oxygen chemisorption on Pt/YSZ [34].

Recent first-principles theoretical investigation of electrochemical promotion using cluster models of oxygen adsorbed on Cu and Pt metal surfaces with coadsorbed positive and negative ions or point charges [53] has confirmed the experimentally observed linear dependence of the O bond strength on metal work function. The theoretically found slope of the binding energy versus $e\Phi$ for the case of atomic oxygen chemisorption on Pt is −0.5 versus −1 measured

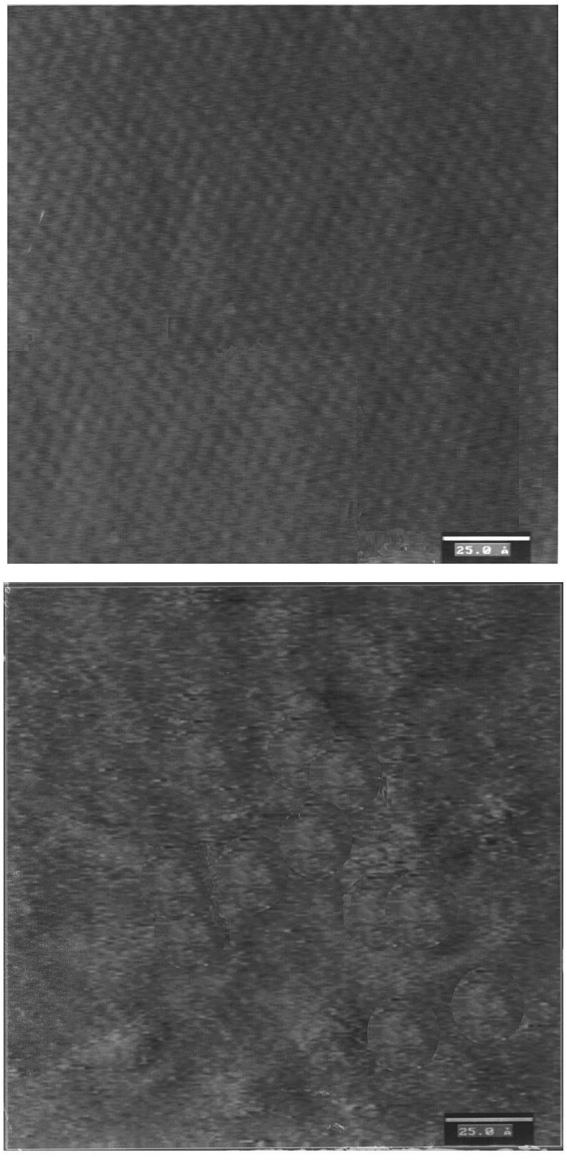

Fig. 11. Atomic resolution STM images (unfiltered) confirming the electrochemically controlled backspillover and spillover of Na on an oxygen-covered Pt(1 1 1) surface of a Pt single crystal interfaced with Na-β''-Al_2O_3 at atmospheric pressure (P_{O_2}=20 kPa) [37]. Top: electrochemically Na-cleaned surface showing the Pt(1 1 1)–(2×2)–O adlattice formed by chemisorbed oxygen. Bottom: electrochemically Na-dosed surface (θ_{Na}=0.01) showing the creation of an ordered Pt(1 1 1)–(12×12)–Na adlattice. Each Na perturbs the electron density of Pt over several atomic distances. (Total scan size 159 Å, V_t=+100 mV, I_t=1.8 nA, reprinted with permission from [37].)

experimentally via TPD [34,53]. This linear relationship was also found at the first-order perturbation theory level by taking into account only the purely electrostatic interaction between the field induced by the ions and the polar metal–oxygen bond. This suggests that the observed pronounced variation in oxygen desorption energy is largely due to electrostatic effects [53], i.e., the «through-the-vacuum» interactions are dominant. In addition to providing a direct explanation for the effect of electrochemical promotion, these results provide a sound theoretical basis for the study and understanding of the role of promoters in heterogeneous catalysis.

4. Conclusions

Electrochemistry can be used to affect the rate and selectivity of heterogeneous catalytic reactions in a reversible and very pronounced manner via the effect of electrochemical promotion or non-Faradaic electrochemical modification of catalytic activity (NEMCA effect). The use of electrokinetic transients, work function measurements, cyclic voltammetry, XPS, TPD and STM has provided conclusive evidence that the effect is due to an electrochemically controlled migration (backspillover) of ionic species ($O^{\delta-}$, in the case of YSZ, $Na^{\delta+}$ in the case of β''-Al_2O_3) from the solid electrolyte onto the gas exposed, i.e. catalytically active, electrode surface.

These ionic species, accompanied by their compensating charge in the metal, thus forming surface dipoles, spread over the entire gas-exposed catalyst–electrode surface and establish an effective electrochemical double layer which affects the binding strength and thus catalytic activity of chemisorbed reactants and intermediates (Fig. 12). Both TPD [34] and isothermal chemisorption studies [56] have shown that, as also manifest by numerous kinetic electrochemical promotion studies [17,18], increasing catalyst potential and work function weakens the chemisorptive bond strength of electron acceptor adsorbates and strengthens the chemisorptive bond strength of electron donor adsorbates. The opposite effects are obtained upon decreasing catalyst potential and work function. This simple rule, also recently confirmed by ab initio quantum mechanical calculations [53] can be used to rationalize practically all the

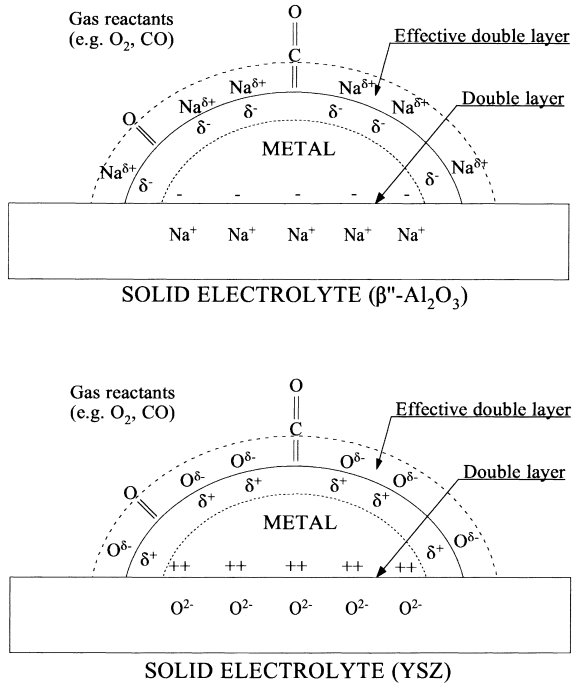

Fig. 12. Schematic representations of a metal electrode deposited on a O^{2-}-conducting and on Na^{+}-conducting solid electrolyte, showing the location of the metal–electrolyte double layer and of the effective double layer created at the metal/gas interface due to potential-controlled ion migration (backspillover).

observed phenomenological features of electrochemical promotion.

The non-Faradaic activation of heterogeneous catalytic reactions via the NEMCA effect is a novel and promising application of electrochemistry. There is a lot of new surface chemistry to be explored [14] with several promising technological possibilities, particularly in industrial product selectivity modification [18] and in exhaust gas treatment [33]. There are still several unresolved scientific and technical issues which will dictate the ultimate industrial usefulness of electrochemical promotion. One of them is the ability to induce NEMCA without external current application by utilizing the catalytic-reaction-driven potential difference between the catalyst and a less active counter electrode [54,55]. Other issues include the ability to induce NEMCA on highly dispersed [30] or on semiconducting catalyst surfaces. Research on these issues is needed to fully understand the technical potential of electrochemical promotion and to estab-

lish the basis for its technological utilization. At the very least, however, the new, electrochemically induced catalytic phenomenon will allow for a systematic study and enhanced understanding of the role of promoters in heterogeneous catalysis.

Acknowledgements

We thank the Electric Power Research Institute (EPRI) and also the PENED programme of the Hellenic Secretariat of Research and Technology for partial financial support.

References

[1] F. Grosz, in: Proceedings of the Second International Symposium on Solid Oxide Fuel Cells, Athens, Greece, CEC, Luxembourg, 1991, pp. 7–24.
[2] S.C. Singhal, H. Iwahara (Eds.), Proceedings of the Third International Symposium on Solid Oxide Fuel Cells, vol. 93–94, The Electrochemical Society, Pennington, NJ, 1993.
[3] W. Göpel, Sensors and Actuators B 18–19 (1994) 1.
[4] C. Wagner, Adv. Catal. 21 (1970) 323.
[5] C.G. Vayenas, H.M. Saltsburg, J. Catal. 57 (1979) 296.
[6] E.J.L. Schouler, M. Kleitz, E. Forest, E. Fernandez, P. Fabry, Solid State Ionics 3–4 (1981) 431.
[7] S. Pancharatnam, R.A. Huggins, D.M. Mason, J. Electrochem. Soc. 122 (1975) 869.
[8] C.G. Vayenas, R.D. Farr, Science 208 (1980) 593.
[9] C.G. Vayenas, S. Bebelis, C.C. Kyriazis, Chemtech 21 (1991) 422.
[10] S. Neophytides, C.G. Vayenas, J. Electrochem. Soc. 137 (1990) 834.
[11] Y. Jiang, I.V. Yentekakis, C.G. Vayenas, Science 264 (1994) 1563.
[12] C.G. Vayenas, S. Bebelis, S. Neophytides, J. Phys. Chem. 92 (1988) 5083.
[13] C.G. Vayenas, S. Bebelis, S. Ladas, Nature (London) 343 (1990) 625.
[14] J. Pritchard, Nature (London) 343 (1990) 592.
[15] J.O'M. Bockris, Z.S. Minevski, Electrochim. Acta 39 (1994) 1471.
[16] B. Grzybowska-Swierkosz, J. Haber, in: Annual Reports on the Progress of Chemistry, vol. 91, The Royal Society of Chemistry, Cambridge, 1994, p. 395.
[17] C.G. Vayenas, S. Bebelis, I.V. Yentekakis, H.-G. Lintz, Catal. Today 11 (1992) 303.
[18] C.G. Vayenas, M.M. Jaksic, S. Bebelis, S. Neophytides, in: J.O'M. Bockris, B.E. Conway, R.E. White (Eds.), Modern Aspects of Electrochemistry, vol. 29, 1996, p. 57.
[19] C. Pliangos, I.V. Yentekakis, S. Ladas, C.G. Vayenas, J. Catal. 159 (1996) 189.
[20] D. Tsiplakides, S.G. Neophytides, O. Enea, M. Jaksic, C.G. Vayenas, J. Electrochem. Soc. 144 (1997) 2072.
[21] S.G. Neophytides, D. Tsiplakides, P. Stonehart, M.M. Jaksic, C.G. Vayenas, Nature (London) 370 (1994) 45.
[22] T.I. Politova, V.A. Sobyanin, V.D. Belyaev, React. Kinet. Catal. Lett. 41 (1990) 321.
[23] L. Basini, C.A. Cavalca, G.L. Haller, J. Phys. Chem. 88 (1994) 10853.
[24] I. Harkness, R.M. Lambert, J. Catal. 152 (1995) 211.
[25] P.C. Chiang, D. Eng, M. Stoukides, J. Catal. 139 (1993) 683.
[26] E. Varkaraki, J. Nicole, E. Plattner, Ch. Comninellis, C.G. Vayenas, J. Appl. Electrochem. 25 (1995) 978.
[27] C.G. Vayenas, S.G. Neophytides, in: Catalysis, vol. 12, The Royal Society of Chemistry, 1996, p. 199.
[28] M. Makri, A. Buekenhoudt, J. Luyten, C.G. Vayenas, Ionics 2 (1996) 248.
[29] C. Pliangos, I.V. Yentekakis, X.E. Verykios, C.G. Vayenas, J. Catal. 154 (1996) 124.
[30] M. Marwood, C.G. Vayenas, J. Catal. 178 (1998) 429.
[31] T. Arakawa, A. Saito, J. Shiokawa, Appl. Surf. Sci. 16 (1983) 365.
[32] S. Ladas, S. Kennou, S. Bebelis, C.G. Vayenas, J. Phys. Chem. 97 (1993) 8845.
[33] A. Palermo, M.S. Tikhov, N.C. Filkin, R.M. Lambert, I.V. Yentekakis, C.G. Vayenas, Stud. Surf. Sci. Catal. 101 (1996) 513.
[34] S. Neophytides, C.G. Vayenas, J. Phys. Chem. 99 (1995) 17063.
[35] C.G. Vayenas, A. Ioannides, S. Bebelis, J. Catal. 129 (1991) 67.
[36] S. Ladas, S. Bebelis, C.G. Vayenas, Surf. Sci. 251–252 (1991) 1062.
[37] M. Makri, C.G. Vayenas, S. Bebelis, K.H. Besocke, C. Cavalca, Surf. Sci. 369 (1996) 351.
[38] S. Bebelis, C.G. Vayenas, J. Catal. 118 (1989) 125.
[39] C. Pliangos, I.V. Yentekakis, X.E. Verykios, C.G. Vayenas, J. Catal. 154 (1995) 124.
[40] C. Cavalca, G.L. Haller, J. Catal. 177 (1998) 389.
[41] C. Karavasilis, S. Bebelis, C.G. Vayenas, J. Catal. 160 (1996) 190.
[42] C.G. Vayenas, S. Bebelis, M. Despotopoulou, J. Catal. 128 (1991) 415.
[43] S. Ladas, S. Kennou, S. Bebelis, C.G. Vayenas, J. Phys. Chem. 97 (1993) 8845.
[44] I.V. Yentekakis, G. Moggridge, C.G. Vayenas, R.M. Lambert, J. Catal. 146 (1994) 293.
[45] C. Karavasilis, S. Bebelis, C.G. Vayenas, J. Catal. 160 (1996) 205.
[46] A. Palermo, R.M. Lambert, I.R. Harkness, I.V. Yentekakis, O. Marina, C.G. Vayenas, J. Catal. 161 (1996) 471.
[47] O.A. Marina, I.V. Yentekakis, C.G. Vayenas, A. Palermo, R.M. Lambert, J. Catal. 166 (1997) 218.
[48] M. Marwood, A. Kaloyannis, C.G. Vayenas, Ionics 2 (1996) 302.
[49] M. Marwood, C.G. Vayenas, J. Catal. 170 (1997) 275.
[50] W. Zipprich, H.-D. Wiemhöfer, U. Vöhrer, W. Göpel, Ber. Bunsengesel. Phys. Chem. 99 (1995) 1406.

[51] C. Cavalca, Ph.D. Thesis, Yale University, 1995.
[52] Y. Jiang, A. Kaloyannis, C.G. Vayenas, Electrochim. Acta 38 (1993) 2533.
[53] G. Pacchioni, F. Illas, S. Neophytides, C.G. Vayenas, J. Phys. Chem. 100 (1996) 16653.
[54] C. Cavalca, G. Larsen, C.G. Vayenas, G.L. Haller, J. Phys. Chem. 97 (1993) 6115.
[55] K. Asano, T. Hibino, H. Iwahara, J. Electrochem. Soc. 142 (1995) 3241.
[56] S. Bebelis, C.G. Vayenas, J. Catal. 138 (1992) 570.